

Spectroscopic and Kinetic Studies of Photochemical Reaction of Magnesium Tetraphenylporphyrin with Oxygen

Jianbin Zhang,^{*,†} Pengyan Zhang,[‡] Zhengfu Zhang,[†] and Xionghui Wei^{*,†}

Department of Applied Chemistry, College of Chemistry & Molecular Engineering, Peking University, Beijing 100190, China, College of Chemical Engineering, Inner Mongolia University of Technology, Huhhot 010051, China

Received: December 18, 2008; Revised Manuscript Received: March 19, 2009

Magnesium tetraphenylporphyrin (MgTPP) was synthesized from *meso*-tetraphenylporphyrin (H₂TPP) in *N,N*-dimethylformamide (DMF). The photochemical properties of MgTPP in the presence of oxygen were investigated in dichloromethane (CH₂Cl₂) by conventional fluorescence, UV–vis, ¹H NMR, MALDI-TOF-MS, FTIR, and XPS spectroscopic techniques. Spectral analyses showed that under irradiation, MgTPP molecules reacted with O₂ molecules, and a stable 1:1 adduct was produced. During the photochemical reaction process, one oxygen molecule was bound to the pyrroline nitrogens in the MgTPP molecule, and the characteristic N–O bonds were identified using the FTIR and XPS techniques. The kinetics of the photochemical reaction of MgTPP with O₂ has been studied in an oxygen-saturated solution. Under irradiation conditions, the experimental rate follows a pseudo-first-order reaction for MgTPP, having a half-life from 40 to 130 min under various irradiation intensities. The kinetic rate constant of photochemical reaction of MgTPP with O₂ showed a linear dependence.

1. Introduction

Chlorophylls and biochlorophylls are compounds that contain magnesium, and they also have important roles in various biological processes. Studies of magnesium-containing porphyrinic compounds have been of interest for a long time.^{1–7} Wróbel and coworkers^{8,9} showed that magnesium porphyrin was a very good compound for light-to-electric energy conversion, but extracted natural chlorophylls from living leaves have seldom been used because of their instability. Chlorophyll *a* in acetone or benzene was irreversibly bleached when exposed to visible light in the presence of O₂.¹⁰ We have recently investigated the reaction of chlorophyll *a* with O₂ under irradiation using fluorescence, UV–vis, and MALDI-TOF MS^{11,12} techniques (*m/z* at 872.5, 893.9, and 927.5) and found that chlorophyll *a* reacts with O₂ rather than accepting it as a ligand. Ligation is of interest because heme and manganese porphyrins play central roles in the activation and transport of O₂ in living organisms.^{13–21}

Oxygen plays a key role in many natural photochemical and photobiological processes such as photooxidation in organic synthesis,²² photodegradation, photoaging and organic synthesis in some biological processes.^{23,24} The transport, storage, and activation of oxygen are the three critical processes for all aerobic life. The detection of molecular oxygen²⁵ is important in many areas such as environmental monitoring and biological, medical, analytical, and industrial chemistry.

Our recent work explored the photochemical reaction of chlorophyll *a* with O₂, and we became especially interested in its function during biochemical oxidation processes. To simplify and simulate the photochemical reaction of chlorophyll *a* with O₂, magnesium tetraphenylporphyrin (MgTPP, Figure 1), which has a porphyrinic framework similar to that of the chlorophylls,

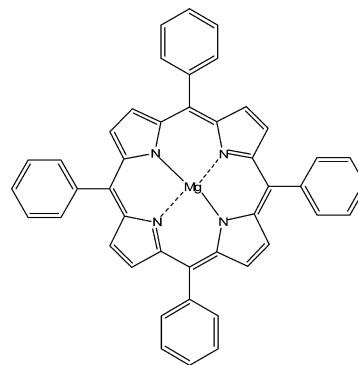


Figure 1. Structure of MgTPP.

was used. Spectral analyses also showed that the reaction of MgTPP with O₂ occurred more efficiently in CH₂Cl₂ under irradiation. The kinetics of photochemical reaction of MgTPP with O₂ has been studied in an oxygen-saturated solution. The photochemical reaction analysis led to a plausible interaction mechanism between a metalloporphyrin and oxygen being postulated, and this may offer new opportunities for the nature of chlorophyll–O₂ interactions associated with intermediates formed during the photocatalysis.

2. Experimental Section

2.1. Instrumentation. Fluorescence spectra were acquired using an F-4500 fluorescence spectrophotometer employing a 500 W Hg–Xe high-pressure lamp. UV–vis spectra were recorded on a Varian CARY 1E UV–vis spectrometer. ¹H NMR spectra were acquired using a Bruker ARX-400 NMR spectrometer, and CDCl₃ was used as NMR solvent. Mass spectra were recorded on Bruker BIFLEX-3 MALDI-TOF mass spectrometer and Bruker APEX IV (7.0 T) Fourier transform ion cyclotron resonance mass spectrometer (FT-ICR-MS). FTIR spectra were acquired as KBr discs on a Bruker VECTOR22

* To whom correspondence should be addressed. Tel: +86-010-62751529. Fax: +86-010-62751529. E-mail: xhwei@pku.edu.cn (X.W.); tadzhang@126.com (J.Z.).

[†] Peking University.

[‡] Inner Mongolia University of Technology.

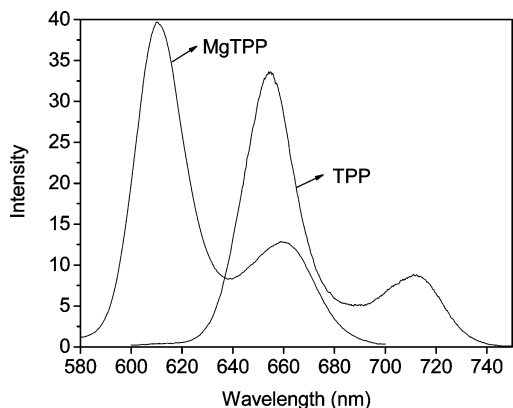


Figure 2. Fluorescence emission ($\lambda_{\text{ex}} = 550 \text{ nm}$) spectra of MgTPP in CH_2Cl_2 and H_2TPP in CH_2Cl_2 .

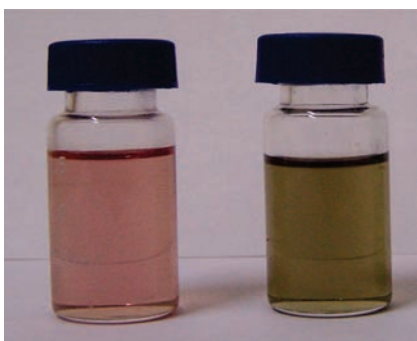


Figure 3. Photograph of the original MgTPP solution (left) and the MgTPP solution after 6 h of irradiation (right) in the presence of O_2 .

FTIR spectrometer. XPS spectra were obtained using a KRATOS Axis ultra X-ray photoelectron spectrometer with a monochromatized Al $K\alpha$ X-ray ($h\nu = 1486.6 \text{ eV}$) operated at 150 W. All solid reagents were weighed using a Sartorius BS224S electric balance.

2.2. Reagents. *meso*-Tetraphenylporphyrin (H_2TPP , >98%) was purchased from Acros Organics (New Jersey). Dichloromethane (HPLC grade, >99.9%) was purchased from Tianjin Siyou (Tianjin, China). All other reagents and solvents were reagent grade and were used as received.

2.3. Preparation of Magnesium Tetraphenylporphyrin. MgTPP was prepared by modification of the methods described elsewhere.^{26–28} We optimized several steps of the MgTPP synthesis. A solution of 65 mg (0.106 mmol) H_2TPP and 152 mg (0.247 mmol) $\text{Mg}(\text{CH}_3\text{COO})_2 \cdot \text{H}_2\text{O}$ in 15 mL of DMF was refluxed for 1 h in a 50 mL single-necked round-bottomed flask; then, 10 mg CH_3COONa was added to the mixture. After 7 h, the metalation was complete, as judged by absorption spectroscopy. The mixture was diluted with 25 mL of CH_2Cl_2 and washed three times with 15 mL of deionized water. The organic layer was dried (Na_2SO_4) and filtered, and upon it, the filtrate was concentrated to ~ 4 to 5 mL. Chromatography on an alumina (200–300 mesh) column ($3 \times 30 \text{ cm}$, poured as a CH_2Cl_2 slurry) with CH_2Cl_2 elution yielded residual H_2TPP . Elution with CH_2Cl_2 :acetone (1:1) afforded fractions that were concentrated and evaporated to dryness under reduced pressure at 433 K for 4 h affording 58 mg MgTPP (85% yield). UV–vis λ_{max} (nm) (CH_2Cl_2): 424, 563, 602.²⁹ Fluorescence emission λ_{max} (nm) (CH_2Cl_2): 608, 665. MALDI-TOF MS (m/z) Calcd for $\text{C}_{44}\text{H}_{28}\text{N}_4\text{Mg}$, 636.2; found, 636.4; ^1H NMR (CDCl_3 , 400 MHz, δ): 7.717, 7.735, 7.749 (12H, *m*, *p*-PhH), 8.218, 8.223, 8.237, 8.240 (8H, *o*-PhH), 8.846 (8H, β -pyrrole).

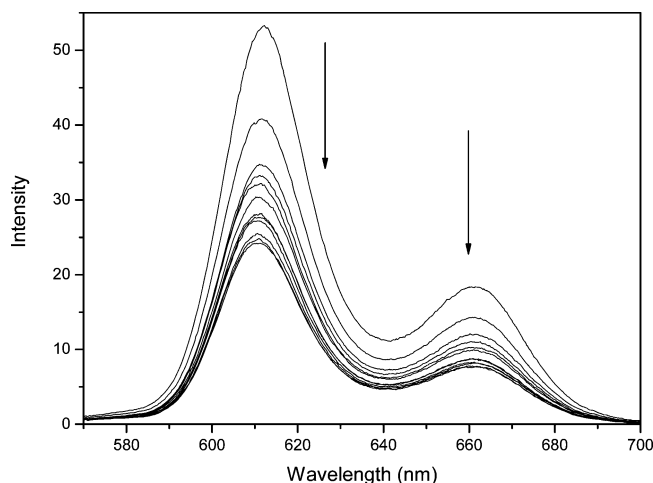


Figure 4. Fluorescence emission ($\lambda_{\text{ex}} = 550 \text{ nm}$) spectral changes of MgTPP under irradiation and in the presence of O_2 .

2.4. Irradiation Processes. A solution of $\sim 35 \text{ mL}$ of MgTPP in CH_2Cl_2 (60 $\mu\text{mol/L}$) was put in a cold trap and irradiated using a 14 W incandescent lamp at a distance of 9 cm. The luminous flux of the lamp was 800 lm at room temperature. Compressed air (99.8% vol) was added to the solution continuously for 6 h so that the photochemical reaction of MgTPP with O_2 could be maintained in an oxygen-saturated solution. Irradiated MgTPP solution (1 mL) was diluted five times with CH_2Cl_2 , and the dilute solutions were used for various spectral analyses every 30 min.

3. Results and Discussion

UV–vis absorption spectra of the H_2TPP solution and the MgTPP solution are shown in the Supporting Information. The absorption spectra show typical Soret bands and several Q bands. The peak at 424 nm was assigned to the Soret band of MgTPP arising from the $a_{1u}(\pi) \rightarrow e_g^*(\pi)$ transition.³⁰ Similar Soret absorption peaks (B bands) are observed for most porphyrinic compounds and are attributed to excitonic interactions between the large Soret transition dipoles of the constituent porphyrin chromophores. The changes in Soret band intensity are very important for the exploration of the photochemical interaction between porphyrinic compounds and other molecules. Compared with H_2TPP , the Soret band maximum of the porphyrin part (P part) of MgTPP is shifted by 7 nm from 417 to 424 nm because the delocalized π bonds of MgTPP increase the average electron density of the porphyrin, which lowers the electron transition energy. The bandwidth of the Soret band in the MgTPP absorption spectrum was similar to that for the reference H_2TPP . Four Q bands of H_2TPP were observed at 513, 548, 594, and 645 nm, whereas, three red-shifted Q bands of MgTPP were observed at 523, 563, and 602 nm. These Q bands of MgTPP are attributed to the $a_{2u}(\pi) \rightarrow e_g^*(\pi)$ transitions.³⁰

The center of the Mg–porphyrin ring is occupied by a Mg ion linked to two pyrrole nitrogens in MgTPP. The Mg ion accepts the lone pair of electrons from the N atoms of the pyrrole rings, whereas electrons from the Mg ion are donated to the porphyrin molecule. Delocalized π bonds are thus formed, which permit the easy flow of electrons within the delocalized π system. Coordination of the Mg ion with N atoms increases the molecular symmetry, and the number of Q bands thus decreases.

Stable-state fluorescence spectra with selective excitation of the MgTPP and H_2TPP moieties were recorded and are shown

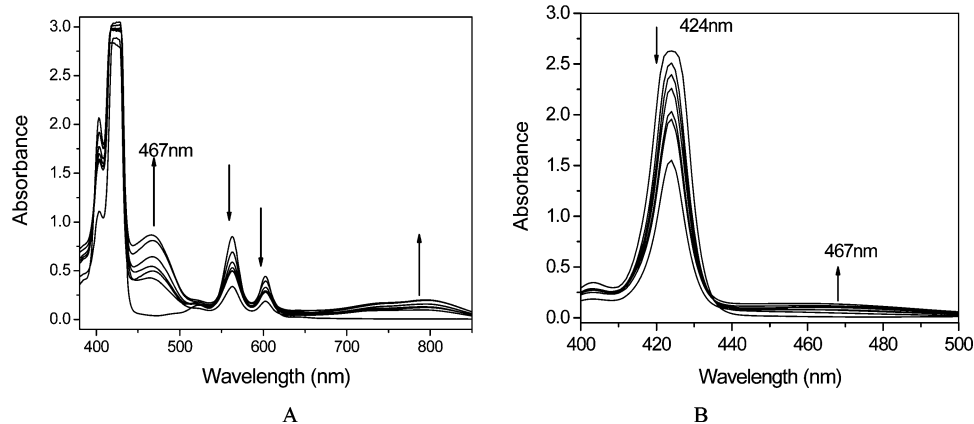


Figure 5. UV-vis absorption spectral changes of the original MgTPP solution in the presence of O_2 that was diluted with CH_2Cl_2 (A) 5 times and (B) 35 times.

in Figure 2. Upon excitation at 550 nm, where the P part of H_2TPP absorbs, strong fluorescence with maximum emission positions of Q^* at 654 and 712 nm were observed. Strong fluorescence for MgTPP with 50 nm blue-shifted maximum emission positions of Q^* at 608 and 665 nm compared with H_2TPP were also observed.

Considering these discussed properties, synthetic MgTPP was used for the following photochemical experiments.

3.1. Contrast Test. The contrast test was performed according to Section 2.4 in the dark. UV-vis absorption spectra and fluorescence emission spectra in the contrast test showed that in the dark, solutions of MgTPP were stable under air for more than a few hours. MALDI-TOF MS spectra showed m/z peaks at 615.4 and 636.7, indicating that no reaction occurred between ground-state MgTPP and O_2 .

3.2. Fluorescence and UV-Visible Spectra. A photograph showing the original MgTPP solution and the MgTPP solution irradiated for 6 h in the presence of O_2 was taken (Figure 3). After irradiation in the presence of O_2 , the color changes of the MgTPP solution from pink to yellowish-brown could be due to a photochemical reaction of MgTPP with O_2 . To confirm the reaction process, the irradiated MgTPP solutions in the presence of O_2 were analyzed by fluorescence and UV-vis spectroscopy every 30 min. These spectra are shown in Figures 4 and 5.

The fluorescence emission spectra (Figure 4) showed a decrease in the fluorescence intensity of the solutions at 605 and 660 nm with increasing irradiation time. The fluorescence of MgTPP was significantly quenched, and this could be attributed to electron transfer taking place from the P part of MgTPP to an acceptor molecule.

UV-vis spectra of the 5-times-diluted solutions (Figure 5A) and 35-times-diluted solutions (Figure 5B) showed that the absorption intensity of the Soret band at 424 nm and the Q bands at 563 and 602 nm decreased with increasing irradiation time. A new Soret band at 467 nm and a new Q band at 793 nm suggest that MgTPP had reacted with O_2 , resulting in the formation of a new compound. An isosbestic point was observed in the UV-vis absorption spectra at 444 nm (Figure 5A). The new Soret band could be due to the reaction of O_2 with the P part of MgTPP.³¹

3.3. Proton Nuclear Magnetic Resonance Spectra. 1H NMR spectra of the original solution of MgTPP in $CDCl_3$ and solutions of MgTPP in $CDCl_3$ that had been irradiated for 3 and 6 h are shown in Figure 6A,B,C. The 1H NMR spectra displayed the characteristic P part and phenyl groups, whereas the appearance of a gradually increasing signal at 7.54 in the

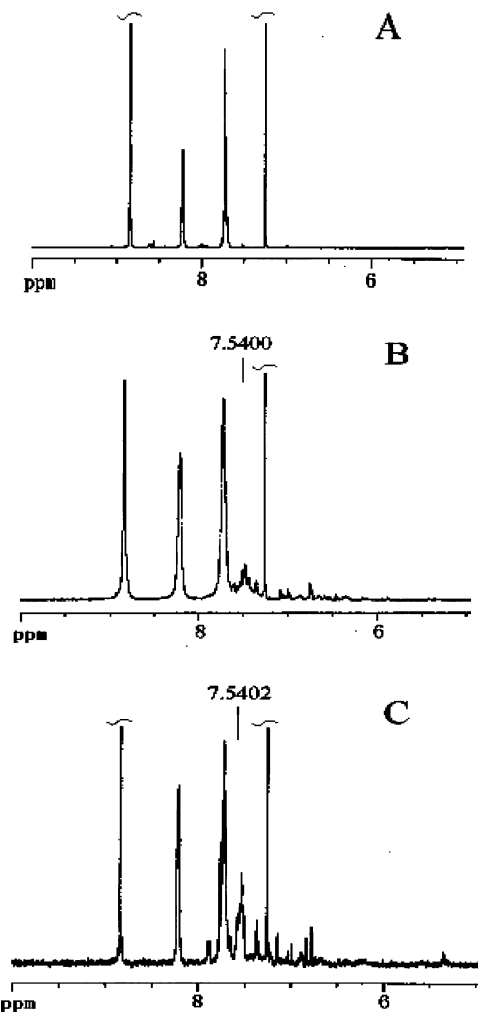


Figure 6. 1H NMR spectral changes of MgTPP solution: (A) original MgTPP in $CDCl_3$, (B) MgTPP in $CDCl_3$ irradiated for 3 h in the presence of O_2 , (C) MgTPP in $CDCl_3$ irradiated for 6 h in the presence of O_2 .

1H NMR spectra was observed as irradiation time increased. These spectra clearly indicated that MgTPP had reacted with O_2 .

3.4. Mass Spectrometry Spectra. MS spectra of the original MgTPP solution and the irradiated MgTPP solution in the presence of O_2 were detected using a MALDI-TOF mass spectrometer, and the spectra are shown in Figure 8A,B.

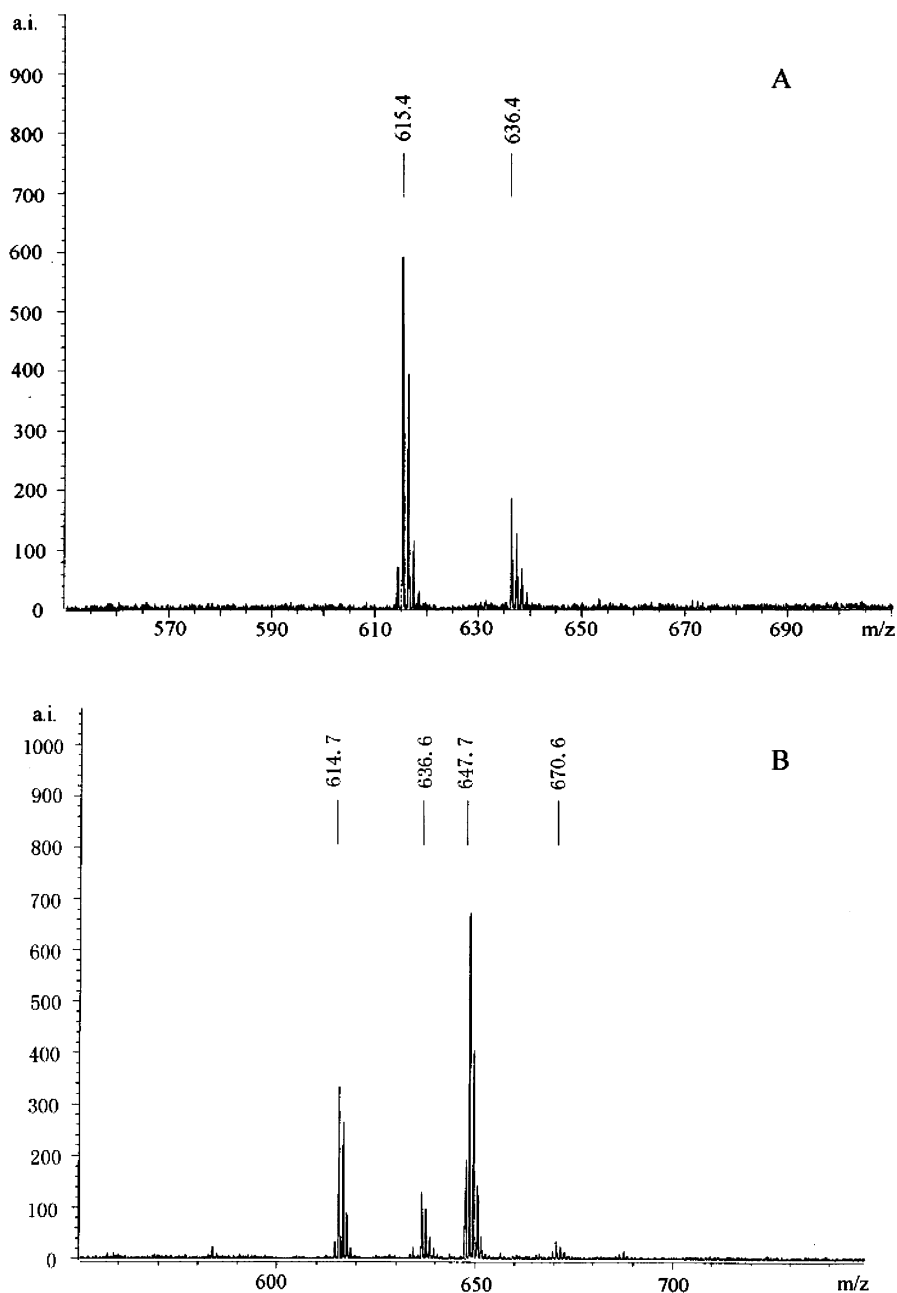


Figure 7. MALDI-TOF MS spectral changes of (A) original MgTPP and (B) irradiated MgTPP in the presence of O₂.

MALDI-TOF MS spectra (Figure 7B) showed four ion peaks of m/z 614.6, 636.6, 647.7, and 670.6. The peak at m/z 614.6 was due to the demagnesium fragment ion peak of MgTPP, the peak at m/z 647.7 was attributed to the demagnesium fragment ion peak of the MgTPP–O₂ complex, and the peak at m/z 670.6 was related to the molecular ion peak of MgTPP–O₂. These spectra indicate that MgTPP reacts with O₂ under irradiation and that the reaction results in the formation of MgTPP–O₂. Accurate MS detection was performed using high-resolution MS, and the spectra showed three peaks at m/z 615.2541, 636.2146, and 647.2427. For the m/z at 647.2427 (M), (M + 1)/M is about 0.50 and (M + 2)/M is about 0.12, so the m/z at 647.2427 can be due to the demagnesium fragment ion peak of the MgTPP–O₂ complex. Meanwhile, the Lederberg law can also prove the result. These mass spectra indicated that one MgTPP molecule had reacted with one oxygen molecule to form a stable 1:1 adduct under irradiation.

3.5. Fourier Transform Infrared Spectroscopy Spectra.

To clarify the bonding sites of MgTPP–O₂, FTIR spectra were obtained to determine possible bonds by analysis of their vibrational bands. The 6-h-irradiated MgTPP solution was evaporated to dryness under reduced pressure at room temperature, and a solid sample was obtained. FTIR spectra of the original and the irradiated MgTPP (Figure 8) were obtained, and several characteristic absorption bands at 1272, 762, and 1203 cm⁻¹ were observed. The absorption band at 1272 cm⁻¹ was due to the stretching vibration of N–O (with a shoulder at 1264–1250 cm⁻¹),³² the absorption band at 762 cm⁻¹ was attributed to the bending vibration of N–O (with a shoulder at 800–780 cm⁻¹),³² and the band at 1203 cm⁻¹ resulted from a characteristic unknown peak,³² which has often been observed in pyridine oxides containing a N–O bond. The exact molecular mechanism of the photochemical reaction of MgTPP with O₂ thus requires further investigation.

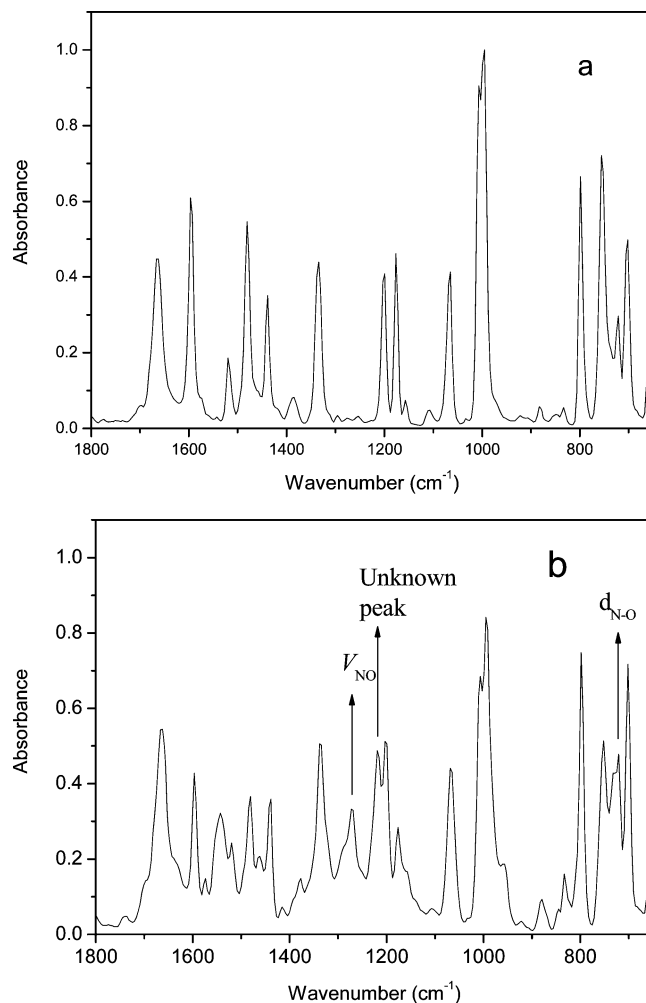


Figure 8. FTIR spectral comparison of (a) MgTPP to (b) MgTPP-O₂.

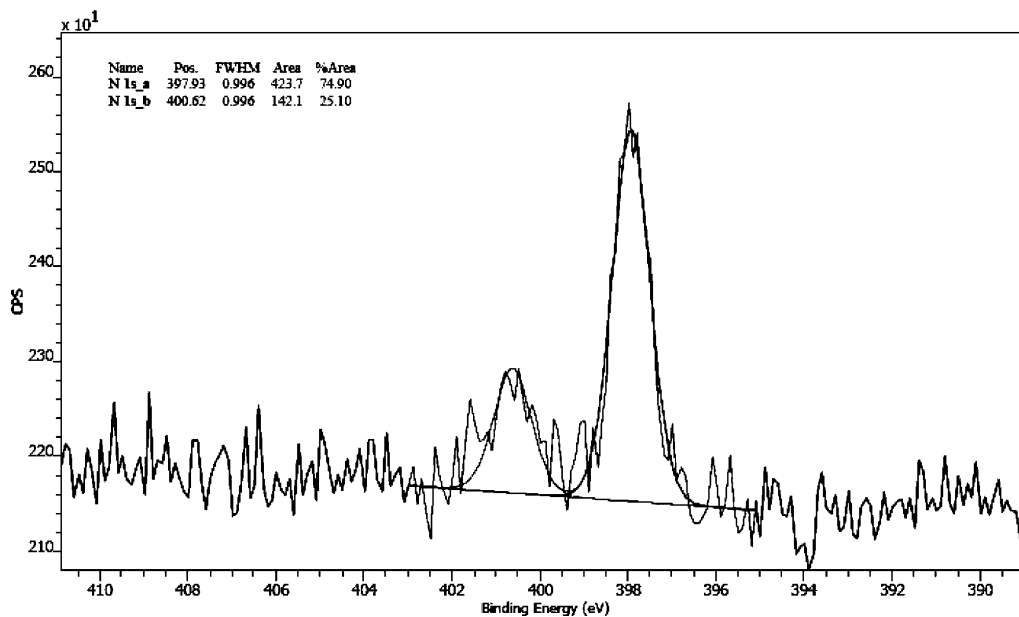


Figure 9. High-resolution N 1s XPS spectra of the solid of MgTPP-O₂ adducts.

3.6. X-ray Photoelectron Spectroscopy (XPS). After photochemical reaction of MgTPP with O₂, the solution was concentrated and evaporated to dryness under reduced pressure, and the solid sample was obtained. The solid was analyzed by the AXIS-HS Kratos instrument to obtain the N (1s) spectra.

The XPS results are shown in Figure 9. The Figure showed that the binding energy of N 1s in the compound was observed at 397.93 eV and 400.62 eV, agreeing with that of NaNO₃, Na₂N₂O₂, and Co(NH₃)₆Cl₃.³³ The binding energy of N 1s at 397.93 eV can be attributed to the ligand N atoms of MgTPP,

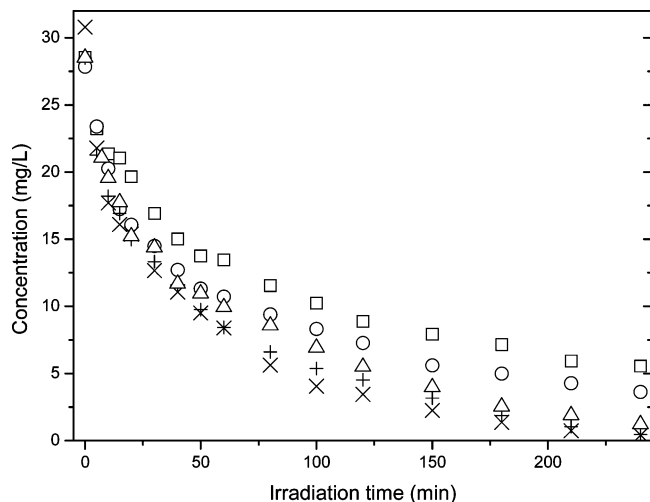


Figure 10. Dependencies of the concentration of MgTPP (mg/L) on irradiation time in CH_2Cl_2 (air flow is 30 mL/min, and the concentration of MgTPP is 30 mg/L): \square , 235 lm; \circ , 400 lm; \triangle , 600 lm; $+$, 800 lm; \times , 930 lm.

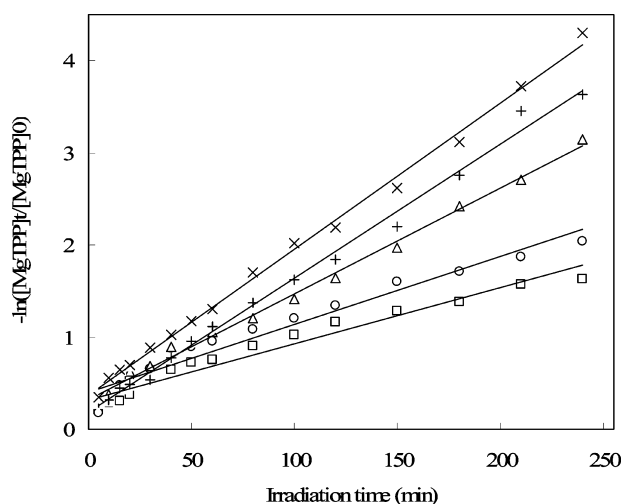


Figure 11. Photochemical reaction kinetics of MgTPP with O_2 at various irradiation intensities: \square , 235 lm; \circ , 400 lm; \triangle , 600 lm; $+$, 800 lm; \times , 930 lm.

which was observed at 397.40 eV ($\text{Na}_2\text{Fe}(\text{CN}^*)_3(\text{NO})$) and 397.90 eV (KOCN).³⁴ The binding energy of N 1s at 400.62 eV can be attributed to the bonding N atoms of MgTPP, which was observed at 402.70 eV ($\text{Na}_2\text{Fe}(\text{CN})_3(\text{N}^*\text{O})$) and 399.30 eV (KOCN).³⁴ XPS analyses show that the N–O bond was formed in the photochemical interaction of MgTPP with O_2 .

3.7. Photochemical Reaction Kinetics. According to the above results, the final product of the MgTPP with oxygen is the species $\text{MgTPP}(\text{O}_2)$ (eq 1). Most reported synthetic O_2 binding systems have been studied in organic solvents such as toluene, benzene, and dichloromethane.^{35–37}



The photochemical reaction rate of MgTPP with O_2 was monitored with the fluorescence technology as a function of irradiation time. A solution of approximately 35 mL of MgTPP in CH_2Cl_2 (30 mg/L) was irradiated using various incandescent lamps with various irradiation intensities at a distance of 9 cm. The luminous flux of the lamp was 220–930 lm at room temperature. Compressed air at 30 mL/min was continuously

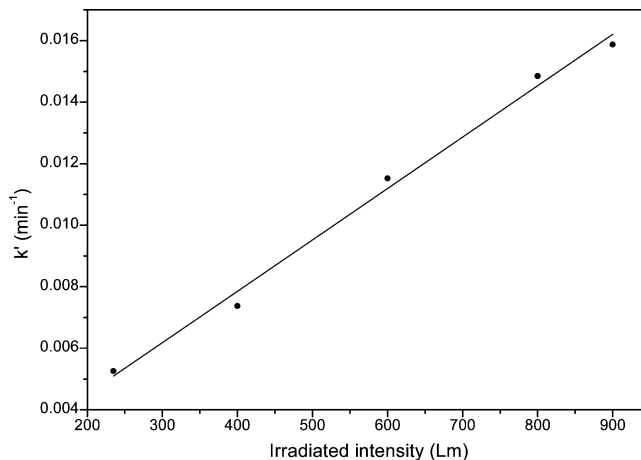


Figure 12. Linear dependencies of the photochemical reaction rate constant on irradiated intensity in CH_2Cl_2 (air flow is 30 mL/min and the concentration of MgTPP is 30 mg/L).

added to the solution for 4 h so that the photochemical reaction of MgTPP with O_2 could be maintained in an oxygen-saturated solution. Irradiated MgTPP solution (1 mL) was diluted five times for various spectral analyses every 5–30 min. The reaction of MgTPP from oxygen is expected to be described by the equation



The kinetic process is described by the equation

$$-d[\text{MgTPP}]/dt = k[\text{MgTPP}][\text{O}_2] \quad (3)$$

where $[\text{MgTPP}]$ denotes the concentration of MgTPP, $[\text{O}_2]$ denotes the concentration of O_2 , t is the reaction time, and k is the rate constant.

When the concentration of O_2 remains constant, the eq 3 is changed into eqs 4–7 as follows

$$-d[\text{MgTPP}]/dt = k'[\text{MgTPP}] \quad (4)$$

$$k' = k[\text{O}_2] \quad (5)$$

$$-\ln([\text{MgTPP}]_t/[\text{MgTPP}]_0) = k't \quad (6)$$

$$t_{1/2} = -\ln 2/k' \quad (7)$$

where $[\text{MgTPP}]_0$ is the initial concentration of MgTPP and $[\text{MgTPP}]_t$ is the concentration of MgTPP at t minutes. A plot of the natural logarithm function on the left as a function of delayed time should yield a straight line with a slope of k' .

Figure 10 shows that when a photochemical reaction took place at various irradiation intensities, the concentration of MgTPP in solution decreased with increasing irradiation time. Furthermore, the concentration of MgTPP in solution obviously decreased at the same irradiation time with increasing irradiation intensities.

The kinetics of the photochemical reaction of MgTPP with O_2 is shown in Figure 11. The Figure shows that MgTPP loss by photochemical reaction follows a pseudo-first-order reaction kinetics. The reaction rate constants and half-life of photochemical reaction are shown in Table 1, together with the correlation coefficients obtained from the linear regression analysis. Figure 11 shows a typical plot of eq 6 from an experiment in which MgTPP is irradiated to various irradiation intensities.

Under these conditions, the experimental photochemical reaction of MgTPP with O_2 has a half-life from 40 to 130 min

TABLE 1: Intercept Values: Pseudo-First-Order Reaction Rate Constants, k' , and Half-Lives, $t_{1/2}$, for MgTPP Reaction with O₂ at Various Irradiation Intensities

irradiation intensity (Im)	235	400	600	800	930
k' (min ⁻¹)	0.00526	0.00737	0.01152	0.01485	0.01587
correlation coefficient (R^2)	0.9817	0.9606	0.9948	0.9939	0.9963
$t_{1/2}$ (min)	131.78	94.05	60.17	46.68	43.68

under various irradiation intensities. The kinetic rate constant of photochemical reaction of MgTPP with O₂ showed a linear dependence to be $k' = 2 \times 10^{-5}$ (irradiation intensity/Im) + 0.00117 (correlation coefficient (R^2) = 0.993) (Figure 12).

4. Conclusions

MgTPP was synthesized using H₂TPP and Mg(CH₃COO)₂ in DMF. The photochemical reaction of MgTPP with O₂ was investigated, and our approach was to simulate the photochemical reaction processes of chlorophyll *a* with O₂. The reaction of MgTPP with O₂ under irradiation led to a 1:1 adduct in which one O₂ molecule was bound to the pyrroline nitrogens of MgTPP. The phenomena are noteworthy, although the reasons are unclear. Under these conditions, the experimental rate was the pseudo-first-order reaction for MgTPP, having a half-life from 40 to 130 min under various irradiation intensities. The kinetic rate constants of photochemical reaction of MgTPP increase from 5.26×10^{-3} to 1.587×10^{-2} min⁻¹ in various irradiation intensities, and these constants showed a linear dependence.

Acknowledgment. This project was financed by Jiangxi Boyuan Industry (Jiangxi province, China). We thank Professor Wenting Hua and Professor Hongcheng Gao (Peking University, China) for their suggestions on the photochemical reaction of MgTPP with oxygen.

Supporting Information Available: UV-vis absorption spectra of H₂TPP in CH₂Cl₂ and MgTPP in CH₂Cl₂. This material is available free of charge via the Internet at <http://pubs.acs.org>.

References and Notes

- O'Shea, D. F.; Miller, M. A.; Matsueda, H.; Lindsey, J. S. Investigation of the Scope of Heterogeneous and Homogeneous Procedures for Preparing Magnesium Chelates of Porphyrins, Hydroporphyrins, and Phthalocyanines. *Inorg. Chem.* **1996**, *35*, 7325–7338.
- Tsutsumi, O.; Hirokazu, S.; Takeda, K.; Ogawa, T. Synthesis and Photochemical Behavior of Metalloporphyrin Complexes Containing a Photochromic Axial Ligand. *Thin Solid Films* **2006**, *499*, 219–223.
- Willigen, H.; Ebersole, M. H. ESR and ENDOR Study of the Photooxidation of Magnesium and Zinc Tetrakis(4-sulfonatophenyl)porphyrins. *J. Am. Chem. Soc.* **1987**, *109*, 2299–2302.
- Miller, J. R.; Dorough, G. D. Pyridinate Complexes of Some Metallo-Derivatives of Tetraphenylporphyrin and Tetraphenylchlorin. *J. Am. Chem. Soc.* **1952**, *74*, 3977–3981.
- Kozlowski, P. M.; Wolinski, K.; Pulay, P. GIAO Nuclear Magnetic Shielding Tensors in Free Base Porphyrin and in Magnesium and Zinc Metalloporphyrins. *J. Phys. Chem. A* **1999**, *103*, 420–425.
- Szulbinski, W. S. A Spectroelectrochemical and Photochemical Investigation of Photoinduced Electron Transfer Reaction Between Mg(II) Porphyrin and Viologen. *Inorg. Chim. Acta* **1995**, *228*, 243–250.
- Zaleski, J. M.; Chang, C. K.; Leroi, G. E.; Cukier, R. I.; Nocera, D. G. Role of Solvent Dynamics in the Charge Recombination of a Donor/Acceptor Pair. *J. Am. Chem. Soc.* **1992**, *114*, 3564–3565.
- Wróbel, D.; Boguta, A.; Ion, R. M. Mixtures of Synthetic Organic Dyes in a Photoelectrochemical Cell. *J. Photochem. Photobiol., A* **2001**, *138*, 7–22.
- Wróbel, D.; Lukasiwica, J.; Henryk, M. Fluorescence Quenching and ESR Spectroscopy of Metallic Porphyrins in the Presence of an Electron Acceptor. *Dyes Pigm.* **2003**, *58*, 7–18.
- Aronoff, S.; Mackinney, G. The Photo-oxidation of Chlorophyll. *J. Am. Chem. Soc.* **1943**, *65*, 956–958.

- Yamauchi, S.; Suzuki, Y.; Ueda, T.; Akiyama, K.; Ohba, Y.; Iwaizumi, M. Fluorescence Studies on the Photo-Induced Ligation in the Excited Singlet State of Magnesium Tetraphenylporphyrin. *Chem. Phys. Lett.* **1995**, *232*, 121–126.
- Srinivasan, N.; Haney, C. A.; Lindsey, J. S.; Zhang, W. Z.; Chait, B. T. Investigation of MALDI-TOF Mass Spectrometry of Diverse Synthetic Metalloporphyrins, Phthalocyanines and Multiporphyrin Arrays. *J. Porphyrins Phthalocyanines* **1999**, *3*, 283–291.
- Fry, H. C.; Hoertz, P. G.; Wasser, L. M.; Karlin, K. D.; Meyer, G. J. Efficient Photodissociation of O₂ from Synthetic Heme and Heme/M (M = Fe, Cu) Complexes. *J. Am. Chem. Soc.* **2004**, *126*, 16712–16713.
- Collman, J. P.; Shiryayev, I. M.; Boulatov, R. Effect of Electron Availability on Selectivity of O₂ Reduction by Synthetic Monometallic Fe Porphyrins. *Inorg. Chem.* **2003**, *42*, 4807–4809.
- Nam, W.; Kim, I.; Lim, M. H.; Choi, H. J.; Lee, J. S.; Jang, H. G. Isolation of an Oxomanganese(V) Porphyrin Intermediate in the Reaction of a Manganese(III) Porphyrin Complex and H₂O₂ in Aqueous Solution. *Chem.—Eur. J.* **2002**, *8*, 2067–2071.
- Szaciłowski, K.; Chmura, A.; Stasicka, Z. Interplay between Iron Complexes, Nitric Oxide and Sulfur Ligands: Structure, (Photo)reactivity and Biological Importance. *Coord. Chem. Rev.* **2005**, *249*, 2408–2436.
- Liu, H. S.; Zhang, L.; Zhang, J. J.; Ghosh, D.; Jung, J.; Downing, B. W.; Whittemore, E. Electrocatalytic Reduction of O₂ and H₂O₂ by Adsorbed Cobalt Tetramethoxyphenyl Porphyrin and Its Application for Fuel Cell Cathodes. *J. Power Sources* **2006**, *161*, 743–752.
- Kim, E.; Shearer, J.; Lu, S. Heme/Cu/O₂ Reactivity: Change in Fe^{III}–(O₂²⁻)–Cu^{II} Unit Peroxo Binding Geometry Effectuated by Tridentate Copper Chelation. *J. Am. Chem. Soc.* **2004**, *126*, 12716–12717.
- Komastu, T.; Matsukawa, Y.; Tsuchida, E. Effect of Heme Structure on O₂-Binding Properties of Human Serum Albumin–Heme Hybrids: Intramolecular Histidine Coordination Provides a Stable O₂-Adduct Complex. *Bioconjugate Chem.* **2002**, *13*, 397–402.
- Komastu, T.; Matsukawa, Y.; Tsuchida, E. Kinetics of CO and O₂ Binding to Human Serum Albumin–Heme Hybrid. *Bioconjugate Chem.* **2000**, *11*, 772–776.
- Collman, J. P.; Yan, Y. L.; Eberspacher, T.; Xie, X.; Solomon, E. Oxygen Binding of Water-Soluble Cobalt Porphyrins in Aqueous Solution. *Inorg. Chem.* **2005**, *44*, 9628–9630.
- Prein, M.; Adam, W. The Schenck Ene Reaction: Diastereoselective Oxyfunctionalization with Singlet Oxygen in Synthetic Applications. *Angew. Chem., Int. Ed. Engl.* **1996**, *35*, 477–494.
- Schweitzer, C.; Schmidt, R. Physical Mechanisms of Generation and Deactivation of Singlet Oxygen. *Chem. Rev.* **2003**, *103*, 1685–1757.
- Ryter, S. W.; Tyrrell, R. M. Singlet Molecular Oxygen (1O₂): A Possible Effector of Eukaryotic Gene Expression. *Free Radical Biol. Med.* **1998**, *24*, 1520–1534.
- Mitra, S.; Foster, T. H. Photochemical Oxygen Consumption Sensitized by a Porphyrin Phosphorescent Probe in Two Model Systems. *Biophys. J.* **2000**, *78*, 2597–2605.
- Choon, O. C.; McKee, V.; Rodley, G. A. The Crystal and Molecular Structure of a Monohydrated Dipicolinate Magnesium Tetraphenylporphyrin Complex. *Inorg. Chim. Acta* **1986**, *123*, L11–L14.
- Kadish, K. M.; Shiue, L. R. Investigation of the Axial Ligand Binding Reactions of (Meso-tetraphenylporphyrinato) Magnesium(II) with Nitrogenous Bases. *Inorg. Chem.* **1982**, *21*, 1112–1115.
- Lindsey, J. S.; Woodford, J. N. A Simple Method for Preparing Magnesium Porphyrins. *Inorg. Chem.* **1995**, *34*, 1063–1069.
- Gerasimchuk, N. N.; Mokhir, A. A.; Rodgers, K. R. Synthesis and Characterization of Dimeric Mutually Coordinated Magnesium meso-2-Pyridylporphyrins. *Inorg. Chem.* **1998**, *37*, 5641–5650.
- Zhang, W. Q.; Shan, N.; Yu, L. X.; Wang, X. Q. UV-visible, Fluorescence and EPR Properties of Porphyrins and Metalloporphyrins. *Dyes Pigm.* **2008**, *77*, 153–157.
- Pandey, A.; Datta, S. N. Theoretical Determination of Standard Oxidation and Reduction Potentials of Chlorophyll-*a* in Acetonitrile. *J. Phys. Chem. B* **2005**, *109*, 9066–9072.
- Xie, J. X.; Chang, J. B.; Wang, X. M. *The Application of Infrared Spectra in Organic Chemistry and Medicinal Chemistry*; Science Press: Beijing, 2002.
- Wang, J. Q.; Wu, W. H.; Feng, D. M. *Introduction to Electron Spectroscopy (XPS/XAES/UPS)*; National Defense Industry Press: Beijing, 1992; pp 550–551.

(34) Sasaki, R. T.; Kanagawa, T.; Ohtsuka, K.; Miura, K. Corrosion products of tin in humid air containing sulfur dioxide and nitrogen dioxide at room temperature. *Corros. Sci.* **2003**, *45*, 847–854.

(35) Collman, J. P.; Boulatov, R.; Sunderland, C. J.; Fu, L. Functional Analogues of Cytochrome *c* Oxidase, Myoglobin, and Hemoglobin. *Chem. Rev.* **2004**, *104*, 561–588.

(36) Collman, J. P.; Fu, L. Synthetic Models for Hemoglobin and Myoglobin. *Acc. Chem. Res.* **1999**, *32*, 455–463.

(37) Ruzie, C.; Even, P.; Ricard, D.; Roisnel, T.; Boitrel, B. O₂ and CO Binding to Tetraaza-Tripodal-Capped Iron (II) Porphyrins. *Inorg. Chem.* **2006**, *45*, 1338–1348.

JP811209K